

N65-88105

(ACCESSION NUMBER)

19

(PAGES)

(THRU)

(CODE)

22

Copy
RM SL54107

(NASA CR OR TMX OR AD NUMBER)

(CATEGORY)

NACA

RESEARCH MEMORANDUM

for the

Bureau of Aeronautics, Department of the Navy

WIND-TUNNEL INVESTIGATION AT LOW SPEED OF THE YAWING

STABILITY DERIVATIVES OF A 1/10-SCALE MODEL

OF THE DOUGLAS A4D-1 AIRPLANE

TED NO. NACA DE 389

By Walter D. Wolhart and H. S. Fletcher

Langley Aeronautical Laboratory
Langley Field, Va.Declassified by authority of NASA,
Classification Change Notices No. 1-1-61
Classified ** 1-1-61DECLASSIFIED - EFFECTIVE 1-15-61
Authority: Memo Geo. Drobka NASA HQ.
Code ATSS-A Dtd. 3-12-64 Subj: Change
in Security Classification Markings

NATIONAL ADVISORY COMMITTEE

FOR AERONAUTICS

WASHINGTON

X-4458

DECLASSIFIED

NATIONAL ADVISORY COMMITTEE FOR AERONAUTICS

RESEARCH MEMORANDUM

for the

Bureau of Aeronautics, Department of the Navy

WIND-TUNNEL INVESTIGATION AT LOW SPEED OF THE YAWING
STABILITY DERIVATIVES OF A 1/10-SCALE MODEL
OF THE DOUGLAS A4D-1 AIRPLANE

TED NO. NACA DE 389

By Walter D. Wolhart and H. S. Fletcher

SUMMARY

An experimental investigation has been made in the Langley stability tunnel to determine the low-speed yawing stability derivatives of a 1/10-scale model of the Douglas A4D-1 airplane. The model was tested in clean and landing configurations with horizontal and vertical tails on and off. The effect of removing the horizontal tail was determined for one of the clean configurations. The effects of external wing stores were determined for one complete clean configuration, for one complete landing configuration, and for one landing configuration with horizontal and vertical tails off. Also included in the investigation were the effects of slats and flaps on the wing-alone derivatives.

These data are presented without analysis in order to expedite distribution.

INTRODUCTION

An important design objective in the development of any airplane is the attainment of acceptable dynamic flight characteristics. Previous experience has indicated that reliable prediction of the dynamic flight characteristics for a wide angle-of-attack range requires more accurate estimates of the various aerodynamic parameters than is possible with the use of available procedures. (See refs. 1 and 2, for example.)

DECLASSIFIED - EFFECTIVE 1-25-64
Authority: Memo Geo. Drobka NASA HQ.
Code ATSS-A Dtd. 3-12-64 Subj: Change
in Security Classification Markings

DECLASSIFIED

The purpose of the present investigation was to determine the yawing stability derivatives of a 1/10-scale model of the Douglas A4D-1 airplane over a wide angle-of-attack range from a series of low-speed tests in the Langley stability tunnel. These tests were made at the request of the Bureau of Aeronautics, Department of the Navy, in order to aid in the development of the Douglas A4D-1 airplane. The results of a previous investigation to determine the static lateral and longitudinal stability characteristics of the same model are given in reference 3.

SYMBOLS

The data presented herein are in the form of standard NACA coefficients of forces and moments which are referred to the stability system of axes with the origin at the center of gravity. The positive direction of forces, moments, and angular displacements are shown in figure 1. The coefficients and symbols are defined as follows:

L	lift, lb
D	drag, lb
Y	side force, lb
M	pitching moment, ft-lb
L'	rolling moment, ft-lb
N	yawing moment, ft-lb
b	span, ft
S	area, sq ft
c	chord, measured parallel to plane of symmetry, ft
\bar{c}	mean aerodynamic chord, $\frac{2}{S} \int_0^{b/2} c^2 dy$
y	spanwise distance from and perpendicular to plane of symmetry, ft
q	free-stream dynamic pressure, $\rho V^2/2$, lb/sq ft

V	free-stream velocity, ft/sec
ρ	mass density of air, slugs/cu ft
α	angle of attack of fuselage reference line, deg
γ	flight-path angle, deg
ϕ	angle of roll, deg
i_t	angle of incidence of horizontal tail with respect to fuselage reference line, deg
δ_f	flap deflection, deg
β	angle of sideslip, deg
ψ	angle of yaw, deg
C_y	lateral-force coefficient, Y/qS_w
C_l	rolling-moment coefficient, $L'/qS_w b_w$
C_n	yawing-moment coefficient, $N/qS_w b_w$
$rb/2V$	yawing angular-velocity parameter, radians
r	yawing angular velocity, $d\psi/dt$, radians/sec

$$C_{y_r} = \frac{\partial C_y}{\partial \frac{rb}{2V}}$$

$$C_{l_r} = \frac{\partial C_l}{\partial \frac{rb}{2V}}$$

$$C_{n_r} = \frac{\partial C_n}{\partial \frac{rb}{2V}}$$

 $\Delta C_{y_r}, \Delta C_{l_r}, \Delta C_{n_r}$

tare increments due to support strut (to be subtracted from basic data)

CONFIDENTIAL

Subscripts:

w	wing
s	wing slats, fully opened
f	split flaps, deflected 50°
c	closed-landing-gear fairings


For convenience, the model components are denoted by the following symbols:

W	wing (when used with subscripts s and f denote slats open and flaps deflected, respectively)
F	ducted fuselage (including canopy)
V	vertical tail
H	horizontal tail
G	landing gear down (when used with subscript c denotes landing gear up and closed-landing-gear fairings)
E	two pylon-mounted external stores

APPARATUS AND MODELS

The tests of the present investigation were made in the 6- by 6-foot test section of the Langley stability tunnel in which curved flight is simulated by curving the airstream about a stationary model (ref. 4). Forces and moments on the model were obtained with the model mounted on a single strut support which was in turn fastened to a conventional six-component balance system.

The model used in this investigation was a 1/10-scale model of the Douglas A4D-1 airplane. Pertinent geometric characteristics of the model are given in figure 2 and table I. Photographs of one of the landing configurations are presented in figure 3. The wing, ducted fuselage, tail surfaces, and external wing stores were constructed primarily of laminated mahogany, although the wing and tail surfaces were built up from a 1/4-inch-thick aluminum-alloy core which provided additional stiffness and metal trailing edges. The plain split flaps and landing-gear doors were made from 1/16-inch thick aluminum sheet and the landing



gear struts were made from brass tubing. The wing leading-edge slats were cast from brass and simulated either a fully opened or fully closed slat position.

TESTS

All the tests were made at a dynamic pressure of 24.9 pounds per square foot which corresponds to a Mach number of about 0.13 and a Reynolds number of 0.99×10^6 based on the wing mean aerodynamic chord of 1.08 feet. The angle-of-attack range for all tests was from approximately -4° to 28° . Tests were made at values of $rb/2V$ of 0, -0.029, -0.061, and -0.080. The various model configurations investigated are shown in table II.

CORRECTIONS

Approximate corrections for jet-boundary effects were applied to the angle of attack by the methods of reference 5. Blockage corrections were determined and applied to the dynamic pressure by the methods of reference 6. These data are not corrected for the effects of the support strut since these effects were determined for only one complete clean configuration and one complete landing configuration. The tares for these two configurations are presented and if applied are to be subtracted from the basic data.

PRESENTATION OF RESULTS

The results of this investigation are presented in figures 4 to 8. For convenience in locating desired information, a summary of the configurations investigated as well as the figures that give data for these

037122-1070

NACA RM SL54107

configurations is given in table III. These data are presented without analysis in order to expedite distribution.

Langley Aeronautical Laboratory,
National Advisory Committee for Aeronautics,
Langley Field, Va., August 25, 1954.

Walter D. Wolhart

Walter D. Wolhart
Aeronautical Research Scientist

H. S. Fletcher

H. S. Fletcher
Aeronautical Research Scientist

Approved:

Thomas A. Harris

Thomas A. Harris
Chief of Stability Research Division

JKS

1 [REDACTED]

REFERENCES

1. Jaquet, Byron M., and Fletcher, H. S.: Lateral Oscillatory Characteristics of the Republic F-91 Airplane Calculated by Using Low-Speed Experimental Static and Rotary Derivatives. NACA RM L53G01, 1953.
2. Campbell, John P., and McKinney, Marion O.: Summary of Methods for Calculating Dynamic Lateral Stability and Response and for Estimating Lateral Stability Derivatives. NACA Rep. 1098, 1952. (Supersedes NACA TN 2409.)
3. Wolhart, Walter D., and Fletcher, H. S.: Wind-Tunnel Investigation at Low Speed of the Static Lateral and Longitudinal Stability Characteristics of a 1/10-Scale Model of the Douglas A4D-1 Airplane - TED No. NACA DE 389. NACA RM SL54H13, Bur. Aero., 1954.
4. Bird, John D., Jaquet, Byron M., and Cowan, John W.: Effect of Fuselage and Tail Surfaces on Low-Speed Yawing Characteristics of a Swept-Wing Model As Determined in Curved-Flow Test Section of the Langley Stability Tunnel. NACA TN 2483, 1951. (Supersedes NACA RM L8G13.)
5. Silverstein, Abe, and White, James A.: Wind-Tunnel Interference With Particular Reference to Off-Center Positions of the Wing and to the Downwash at the Tail. NACA Rep. 547, 1936.
6. Herriot, John G.: Blockage Corrections for Three-Dimensional-Flow Closed-Throat Wind Tunnels, With Consideration of the Effect of Compressibility. NACA Rep. 995, 1950. (Supersedes NACA RM A7B28.)

TABLE I.- GEOMETRIC CHARACTERISTICS

Wing:

Aspect ratio	2.91
Taper ratio	0.226
Quarter-chord sweep angle, deg	33.21
Dihedral angle (trailing edge), deg	2.670
Geometric twist, deg	0
Incidence at root chord (parallel to fuselage reference line), deg	0
Airfoil section (parallel to fuselage reference line)	
Root	Modified NACA 0008
Tip	Modified NACA 0005
Chord (parallel to fuselage reference line), ft	
Root	1.550
Tip	0.350
Area, sq ft	2.600
Span, ft	2.750
Mean aerodynamic chord, ft	1.080

Horizontal tail:

Aspect ratio	2.80
Taper ratio	0.225
Quarter-chord sweep angle, deg	34.37
Dihedral angle, deg	0
Airfoil section (parallel to fuselage reference line)	
Root	Modified NACA 0007
Tip	Modified NACA 0004
Chord (parallel to fuselage reference line), ft	
Root	0.667
Tip	0.150
Area, sq ft	0.459
Span, ft	1.133
Mean aerodynamic chord, ft	0.466
Tail length (distance from center of gravity to $\bar{c}/4$ of tail), ft	1.607

Vertical tail:

Aspect ratio	1.24
Taper ratio	0.195
Quarter-chord sweep angle, deg	42.00
Airfoil section (parallel to fuselage reference line)	
Root	Modified NACA 0007
Tip	Modified NACA 0004
Chord (parallel to fuselage reference line), ft	
Root (measured 1.96 in. above fuselage reference line)	1.069
Tip	0.208
Area, sq ft	0.500
Span, ft	0.786
Mean aerodynamic chord, ft	0.738
Tail length (distance from center of gravity to $\bar{c}/4$ of tail), ft	1.420

Fuselage:

Maximum width, ft	0.533
Maximum depth, ft	0.500
Length, ft	3.703
Cross-sectional area of duct, sq ft	
Inlet (both sides)	0.0343
Exit	0.0179

Lift increasing devices:

Wing flaps:

Type	Split
Maximum deflection, deg	50
Actual span (one side), ft	0.592
Chord (parallel to fuselage reference line), ft	0.208

Wing leading-edge slats:

Slat rotation about hinge line for fully opened position, deg	24
Actual span (perpendicular to fuselage reference line) (one side), ft	0.750
Chord (parallel to fuselage reference line), ft	
Root	0.181
Tip	0.087

DECLASSIFIED

TABLE II.- MODEL CONFIGURATIONS INVESTIGATED

Components	Landing gear	Slats	i_t , deg	Stores
Clean configuration; $\delta_f = 0^\circ$				
WFG_cVH	Up	Closed	0	Off
WFG_cVHE	Up	Closed	0	On
W_sFG_cVH	Up	Open	-4	Off
WFG_cV	Up	Closed	--	Off
WFG_c	Up	Closed	--	Off
W_sFG_c	Up	Open	--	Off
W	--	Closed	--	---
W_s	--	Open	--	---
Landing configuration; $\delta_f = 50^\circ$				
W_fFGVH	Down	Closed	-12	Off
$W_{sf}FGVH$	Down	Open	-12	Off
$W_{sf}FGVHE$	Down	Open	-12	On
W_fFG	Down	Closed	---	Off
$W_{sf}FG$	Down	Open	---	Off
$W_{sf}FGE$	Down	Open	---	On
W_f	----	Closed	---	---
W_{sf}	----	Open	---	---

TABLE III.- SUMMARY OF MODEL CONFIGURATIONS
TESTED AND DATA PRESENTED

Model configuration	Data presented	Figure
$WFG_CVH; i_t = 0^\circ$ WFG_CV $W_{sFG_CVH}; i_t = -4^\circ$ $W_{fFGVH}; i_t = -12^\circ$ $W_{sfFGVH}; i_t = -12^\circ$	Effect of high lift devices on complete configurations; C_{y_r} , C_{n_r} , and C_{l_r} plotted against α	4
$WFG_CVHE; i_t = 0^\circ$ $W_{sfFGVHE}; i_t = -12^\circ$ W_{sfFGE}	Effect of wing stores on a complete clean configuration, a complete landing configuration, and a landing configuration with tails off; C_{y_r} , C_{n_r} , and C_{l_r} plotted against α	5
WFG_C W_{sFG_C} W_{fFG} W_{sfFG}	Effect of high lift devices on tail-off configurations; C_{y_r} , C_{n_r} , and C_{l_r} plotted against α	6
W W_s W_f W_{sf}	Effect of high lift devices on wing alone; C_{y_r} , C_{n_r} , and C_{l_r} plotted against α	7
$WFG_CVH; i_t = 0^\circ$ $W_{sfFGVH}; i_t = -12^\circ$	Tare increments due to support strut for complete clean and complete landing configurations; ΔC_{y_r} , ΔC_{n_r} , and ΔC_{l_r} plotted against α	8

DECLASSIFIED

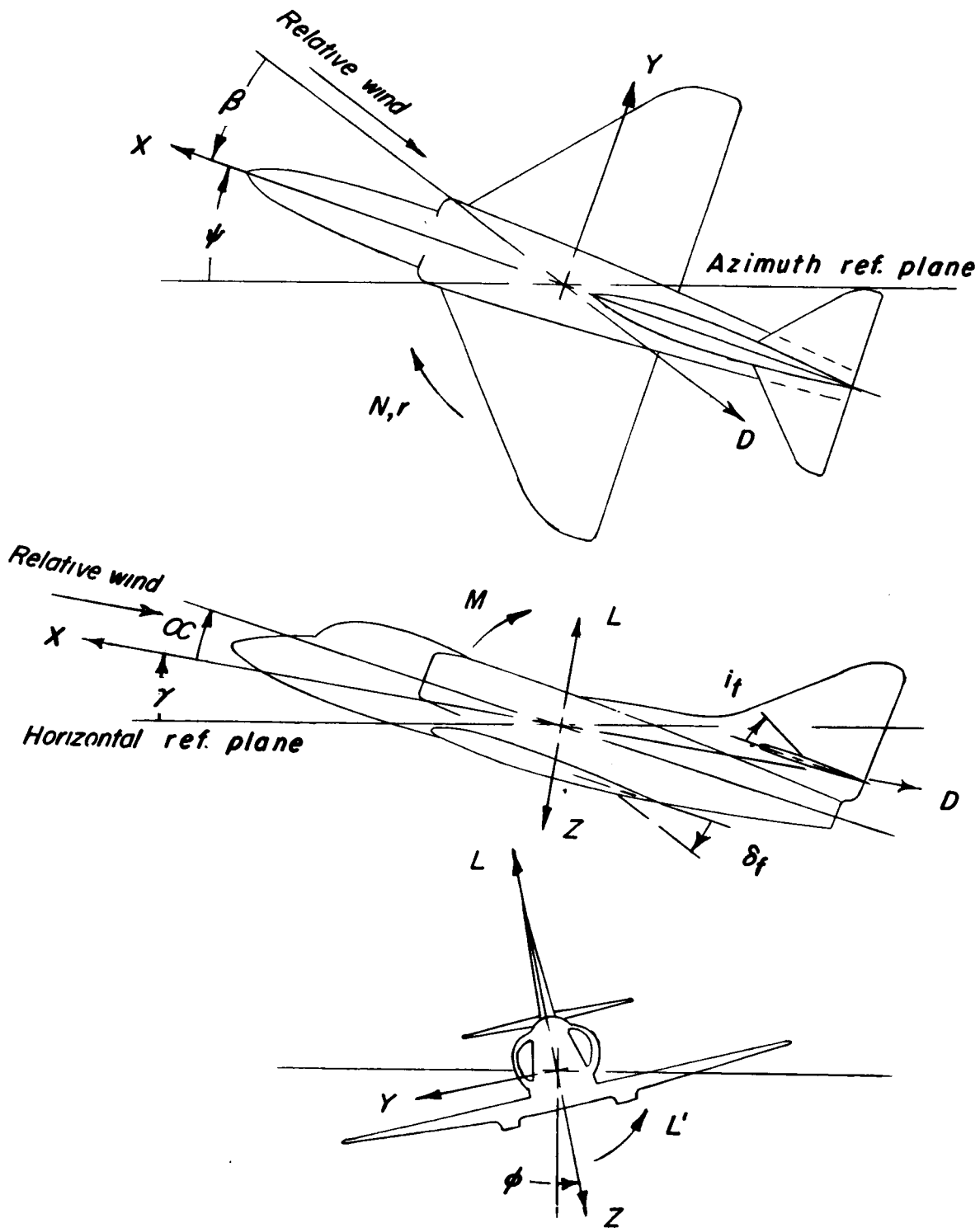


Figure 1.- Stability system of axes. Arrows indicate positive direction of forces, moments, angular displacements, and angular velocities.

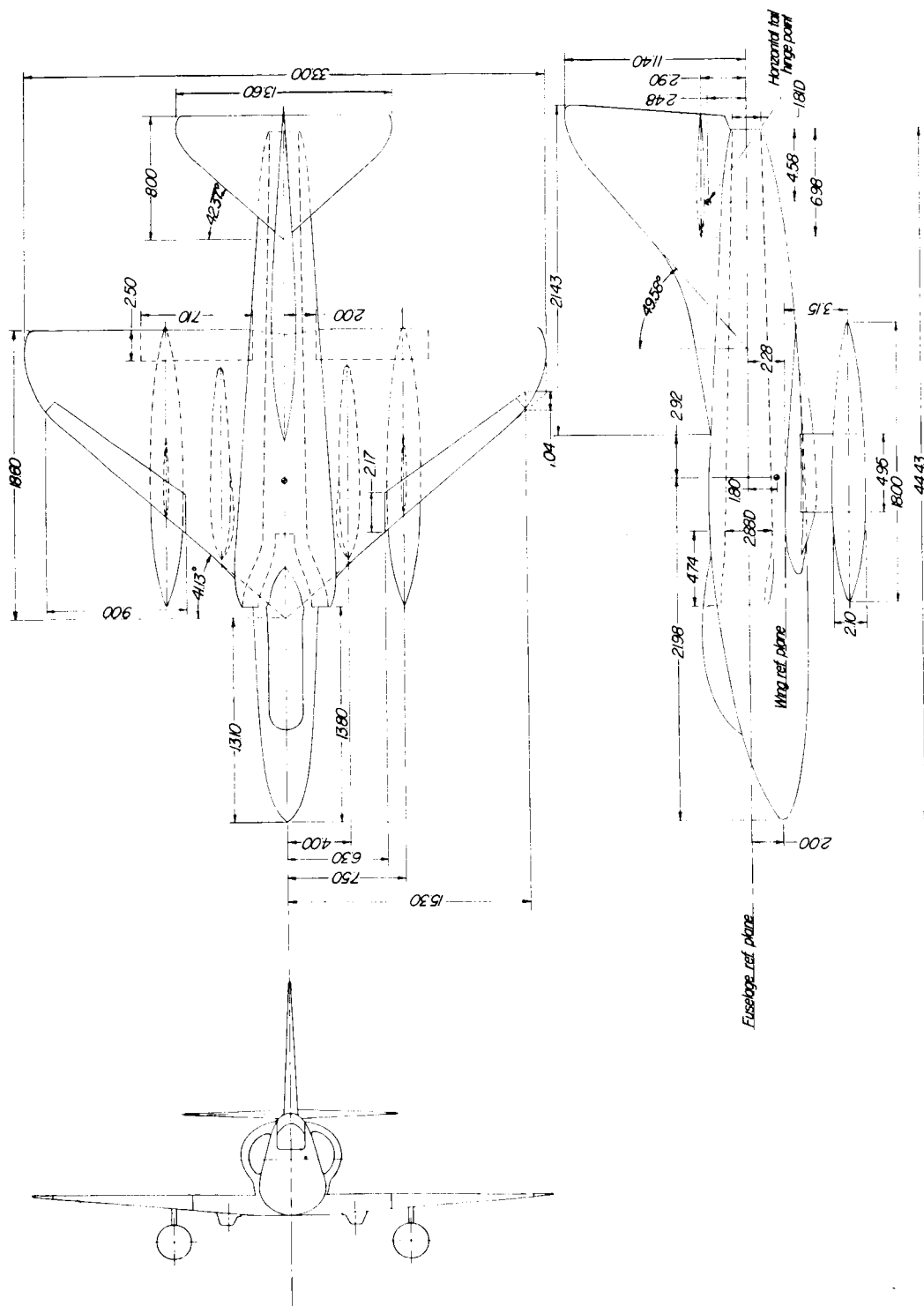
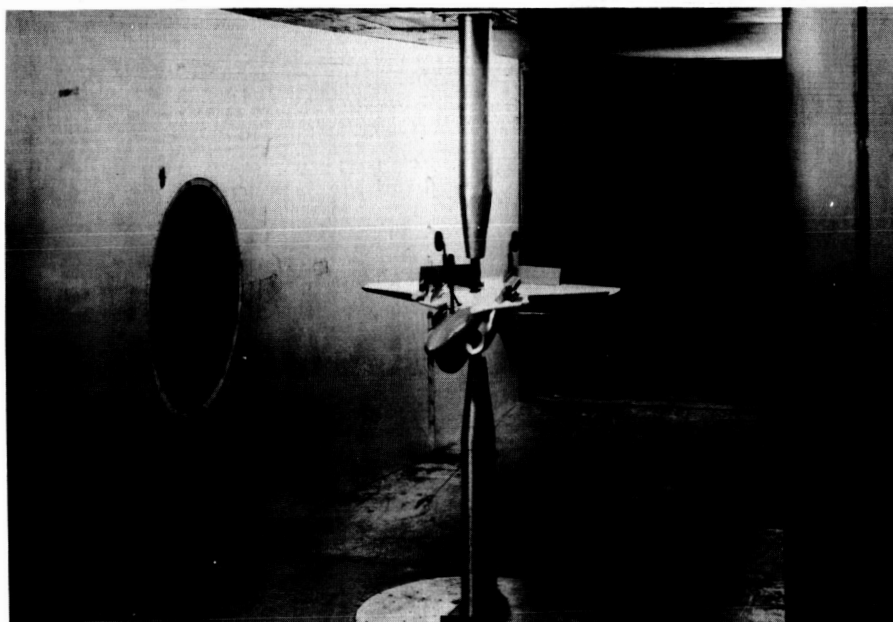


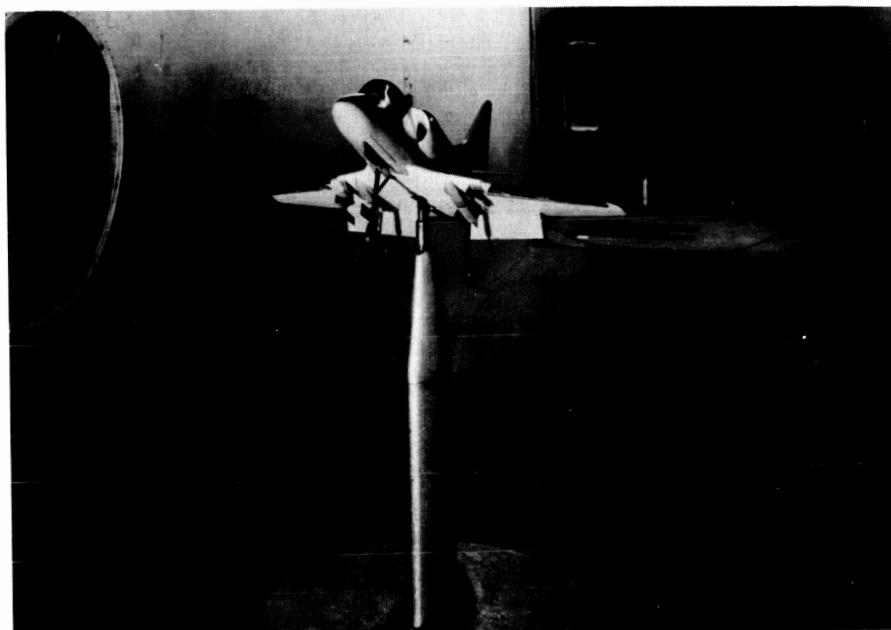
Figure 2.- Geometric characteristics of 1/10-scale model of the Douglas A4D-1 airplane.
All dimensions are in inches.

DECLASSIFIED



L-84446

(a) Three-quarter front view of inverted model with dummy strut in place.



L-84445

(b) Three-quarter front view of erect model.

Figure 3.- Photographs of complete model-landing configuration mounted in the curved-flow test section of the Langley stability tunnel.
 $W_{SF}FGVH$ configuration; $i_t = -12^\circ$.

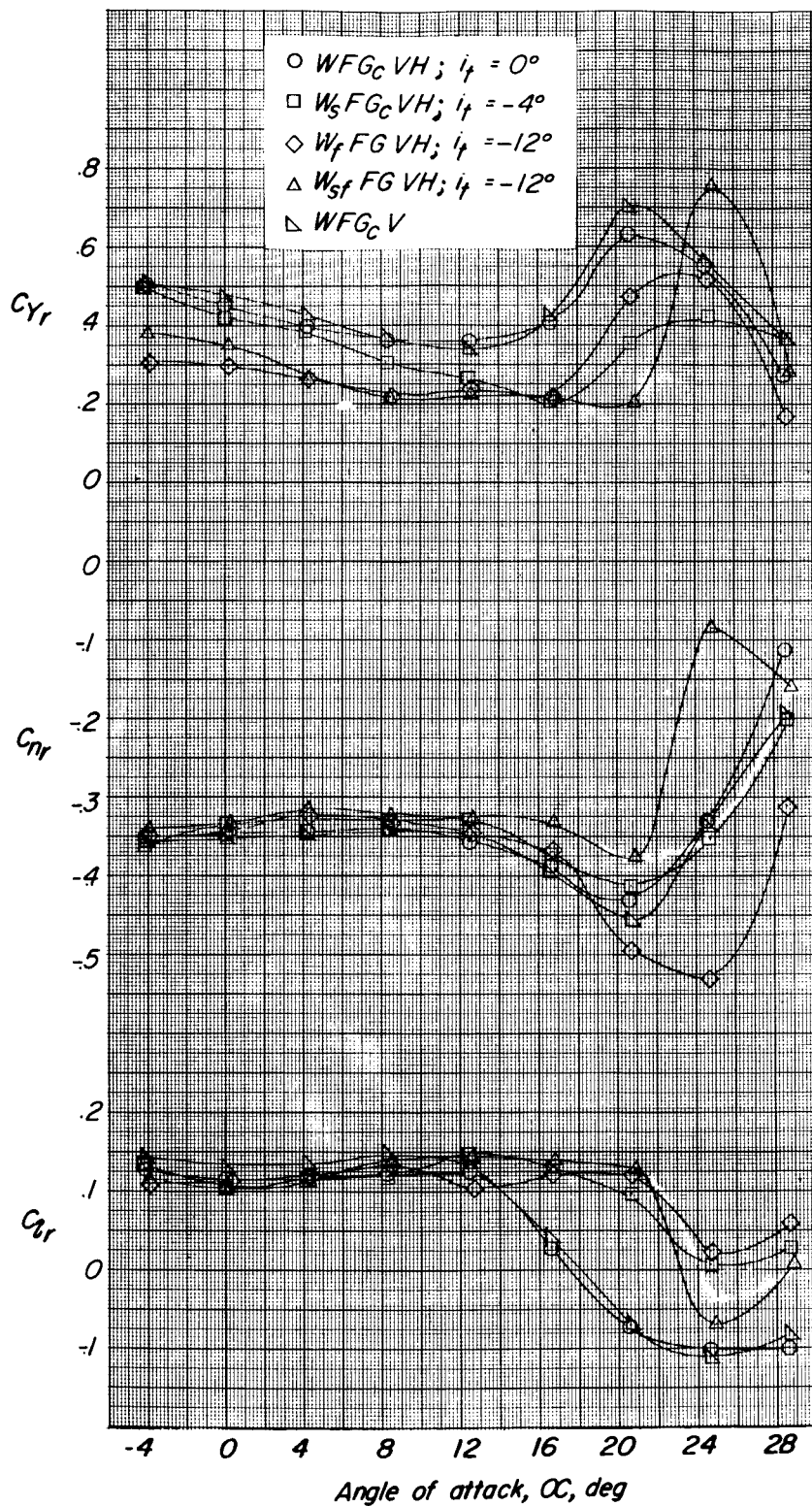


Figure 4.- Effect of horizontal tail and high lift devices on yawing stability derivatives of complete model.

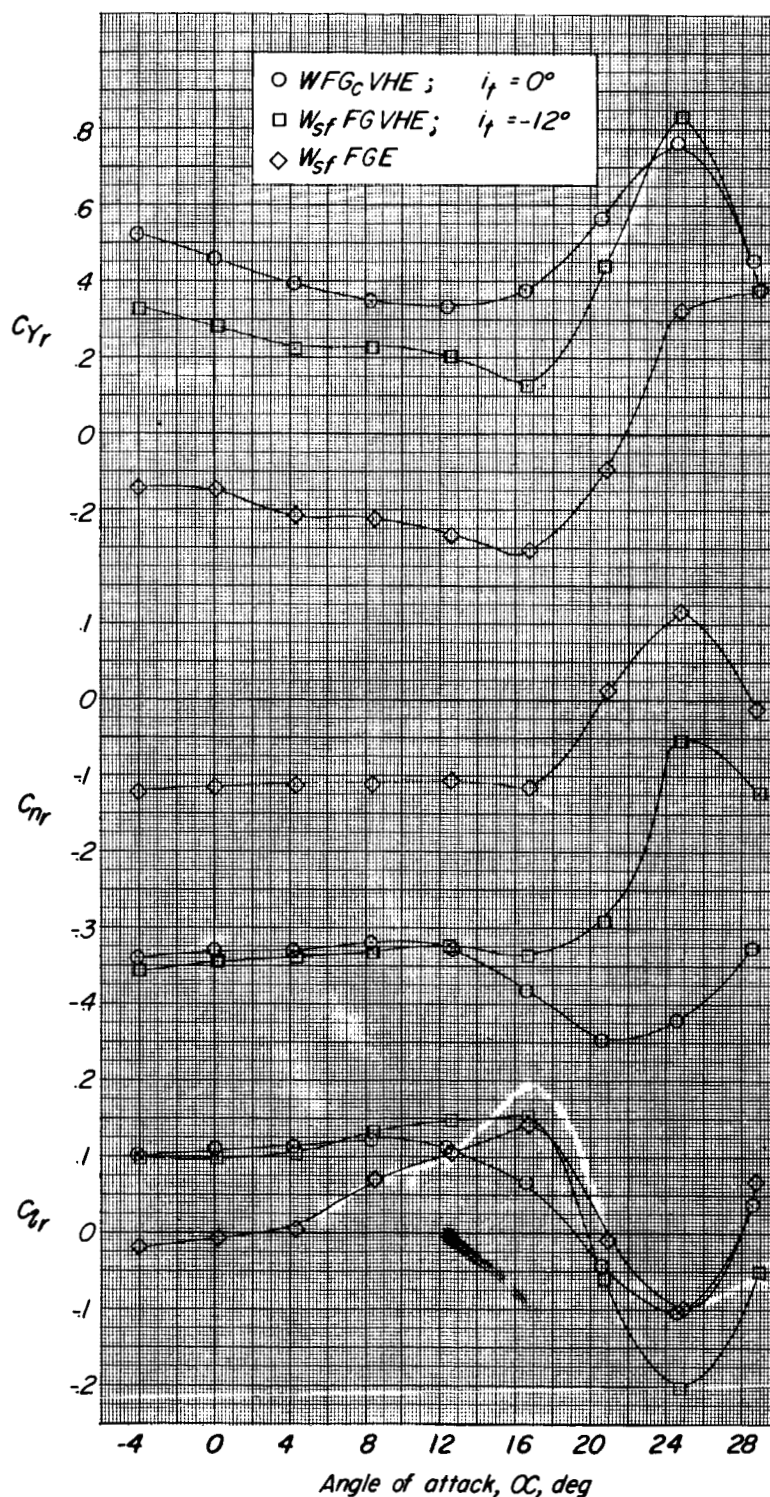


Figure 5.- Effect of wing stores on yawing stability derivatives of complete model-clean configuration, complete model landing configuration, and landing configuration with horizontal and vertical tails off.

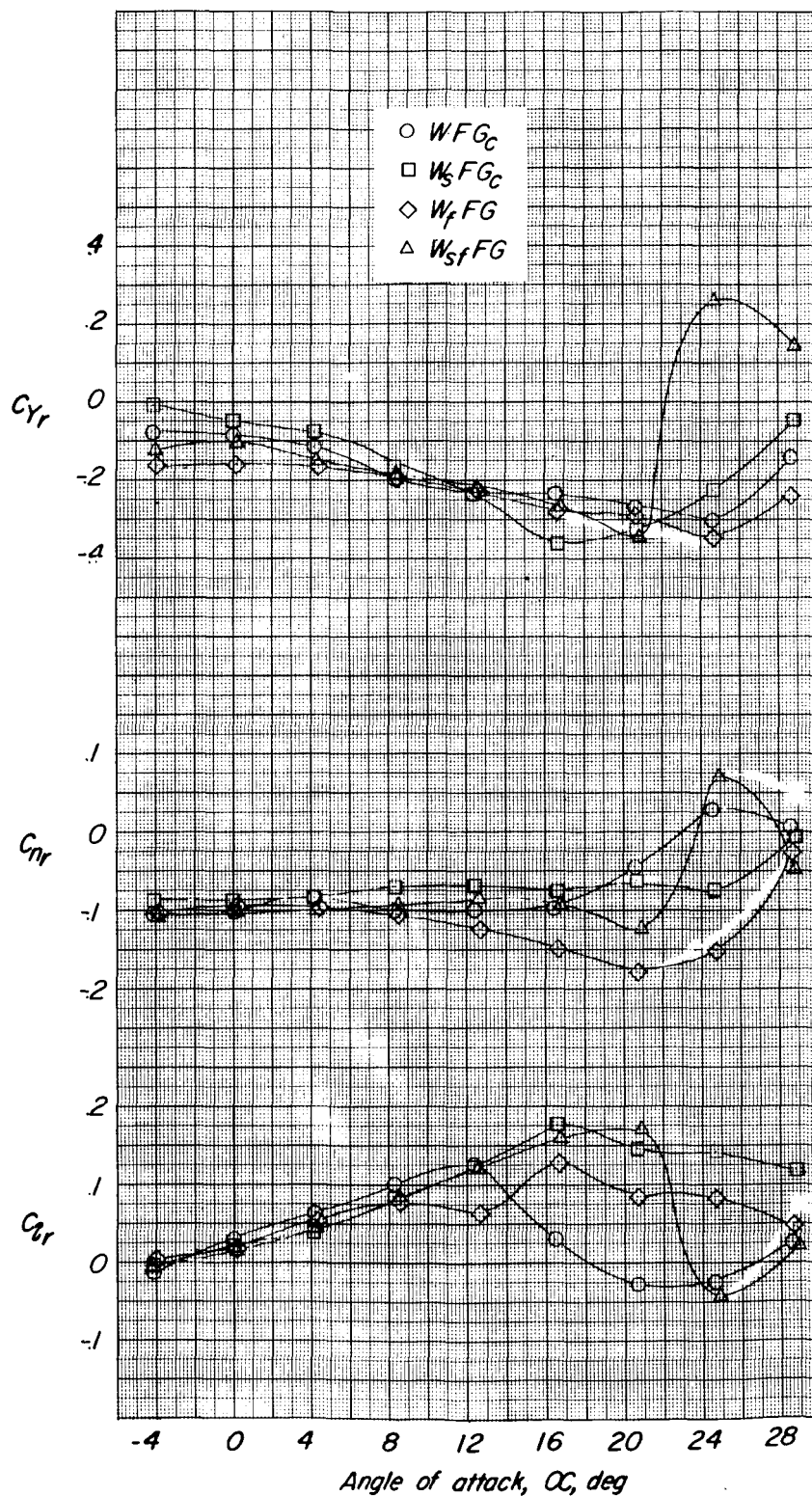


Figure 6.- Effect of high lift devices on yawing stability derivatives of horizontal and vertical tail-off configurations.

SECRET

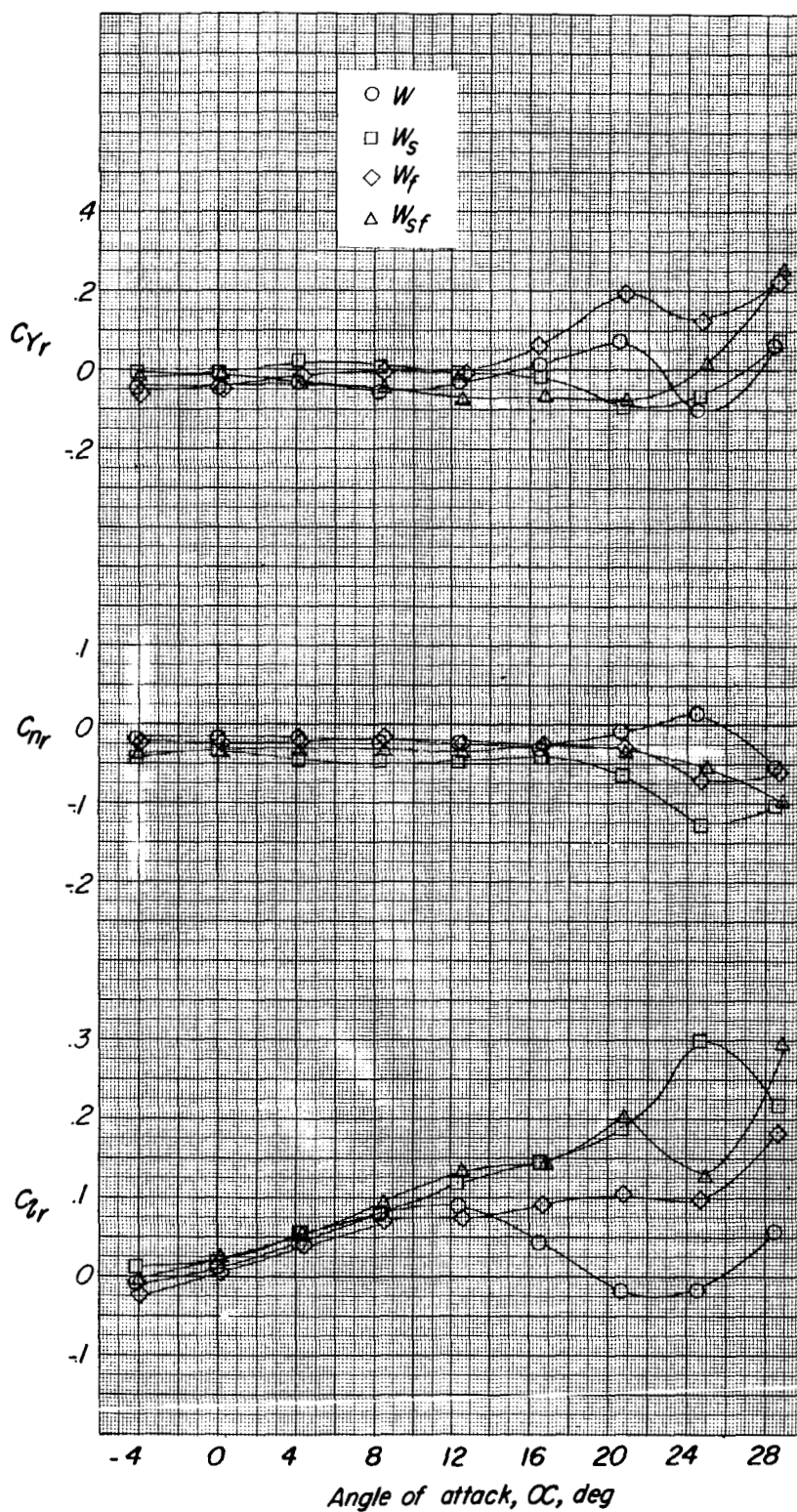


Figure 7.- Effect of high lift devices on yawing stability derivatives of wing alone.

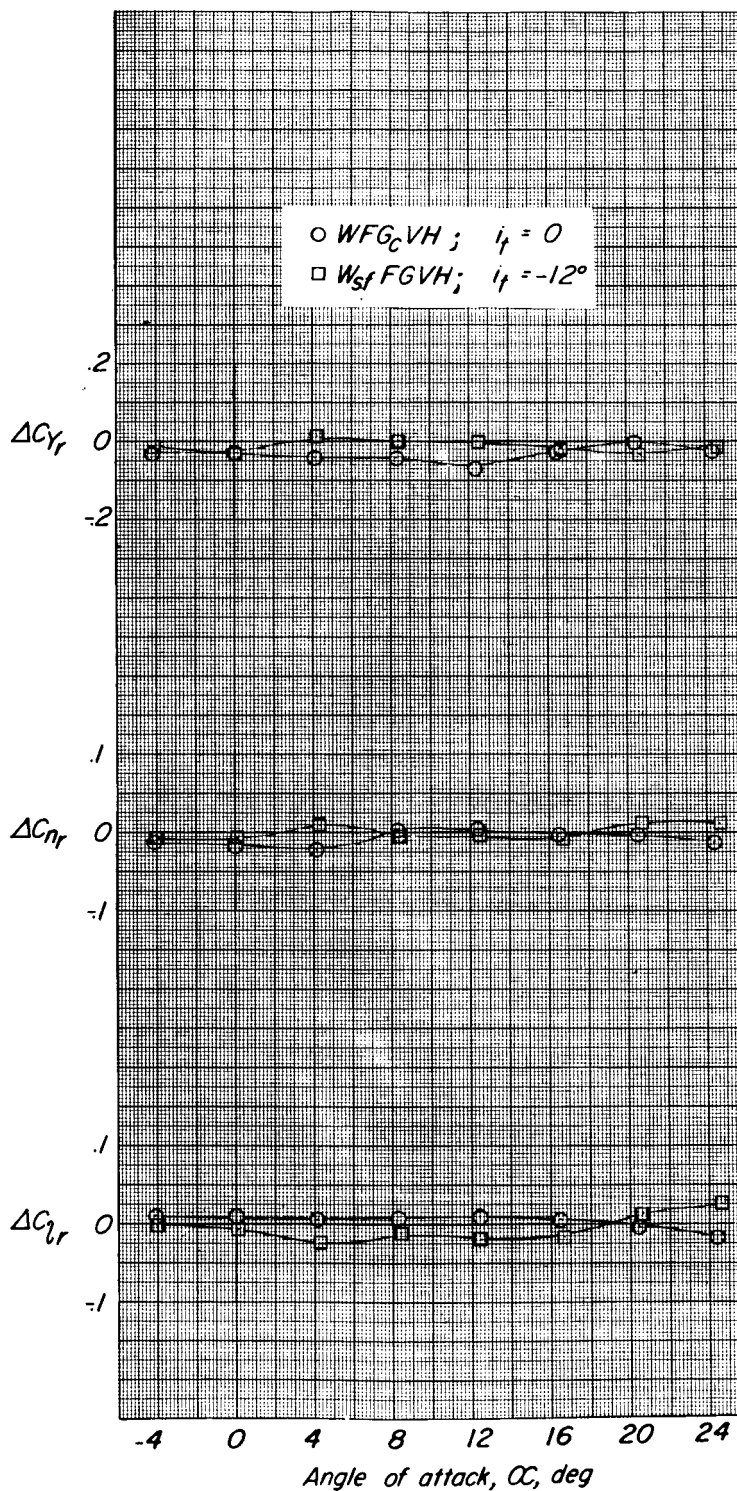


Figure 8.- Support-strut tare increments ΔC_{yr} , ΔC_{nr} , and ΔC_{lr} plotted against α for complete model-clean configuration and complete model-landing configuration.